Supporting Information (SI)

Development of highly-sensitive CNT-metal graphene hybrid Nano-IDA electrochemical biosensor for diagnosis of Alzheimer's disease

M. Mahabubur Rahman[1], Bappa Sarkar[1], Md Tareq Rahman[1], Gyeong J Jin[1], M. Jalal Uddin[1,2], Nabil H. Bhuiyan[1] and Joon S. Shim[1,2,*]

[1]Bio IT Convergence Laboratory, Department of Electronic Convergence Engineering, KwangWoon University, Seoul 01897, Republic of Korea.

[2]NanoGenesis Inc., 20 KwangWoon-ro, Nowon-gu, Seoul 01897, Republic of Korea.

[*]Corresponding author: Joon S. Shim, **Email:** shim@kw.ac.kr, Tel.: +82-10-940-8671

1. Electrochemical ELISA (e-ELISA) Circuit for chronoamperometry analysis

An electrochemical detection circuit has been developed to facilitate the electrochemical reaction utilizing the four electrodes to detect redox species using chronoamperometry. The major functions of the developed electrochemical circuit are to provide the appropriate oxidation and reduction potentials to the IDA working electrodes, applying the potential to the reference electrode to keep the solution's potential stable, allowing the counter electrode to make electrical contact with the solution to complete the electrochemical cell, and detecting and amplifying the sensor current generated throughout the redox reaction.[1, 2] The potential at WE2 can alternate between the ground and the reduction potential provided by the voltage supply. Similarly, the potential at WE1 can alternate between the ground and the oxidation potential through the connection to AMP-1, as shown in **Fig. S1**. The Ag/AgCl reference electrode (RE) is connected to the inverting terminal of Op-amp-2, which is fixed at the ground by grounding the non-inverting terminal. To avoid current flowing through RE and producing potential movement, the CE is connected to Op-amp-2's output.

The output voltage from the amplifier was measured and overall, I-V conversion is given by the equation I= V/R. The output voltage from the detection circuit was recorded with a digital oscilloscope (Analog Discovery 2, was purchased from Digilent Henley Court Pullman, United States).
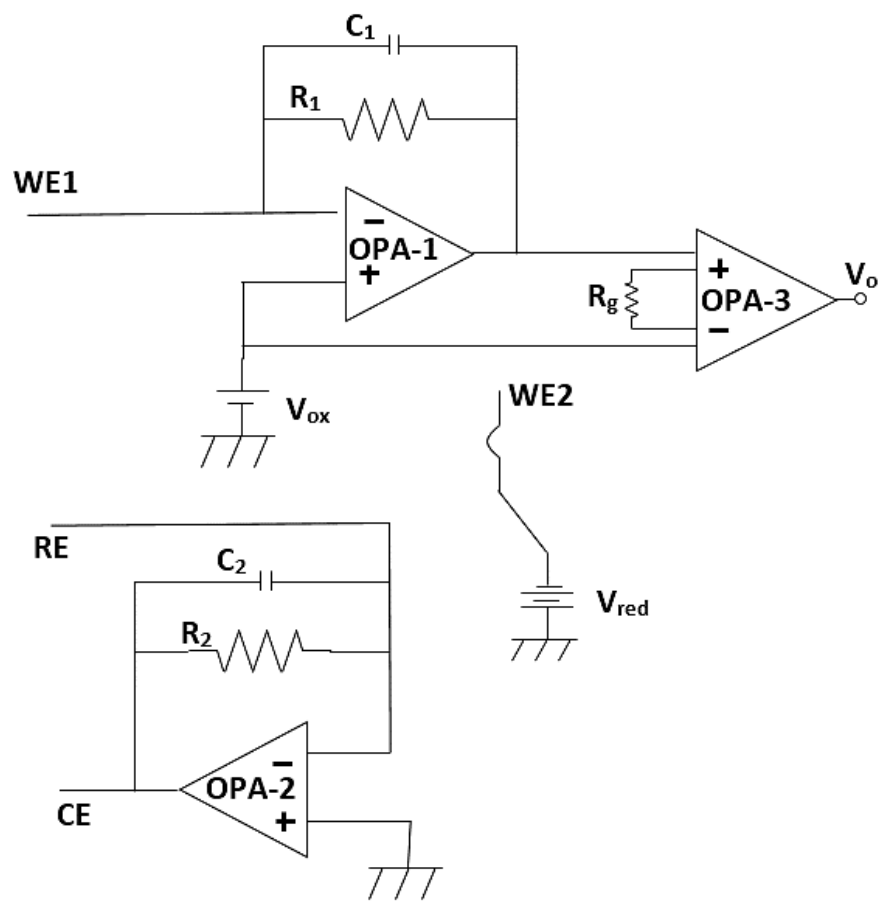
Fig.S1: Schematic Circuit diagram of e-ELISA for chronoamperometry analysis of redox species at IDA electrode.
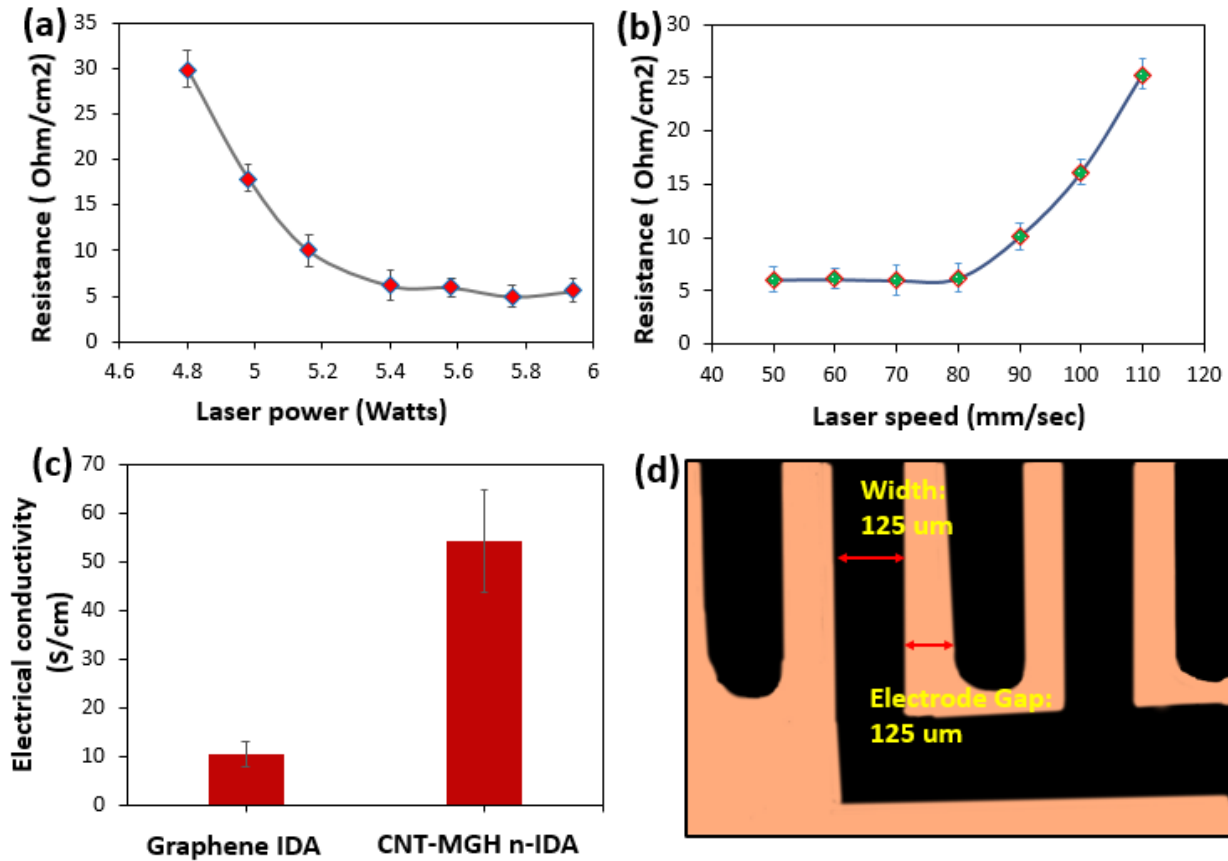
Fig. S2: Optimization of the CO2 laser power and speed, **(a-b)** Resistance changes according to the laser power and laser speed, **(c)** Measured electrical conductivity for graphene IDA and CNT-MGH n-IDA, **(f)** microscope image of the proposed sensor showing the gap between two electrodes and the electrode width.

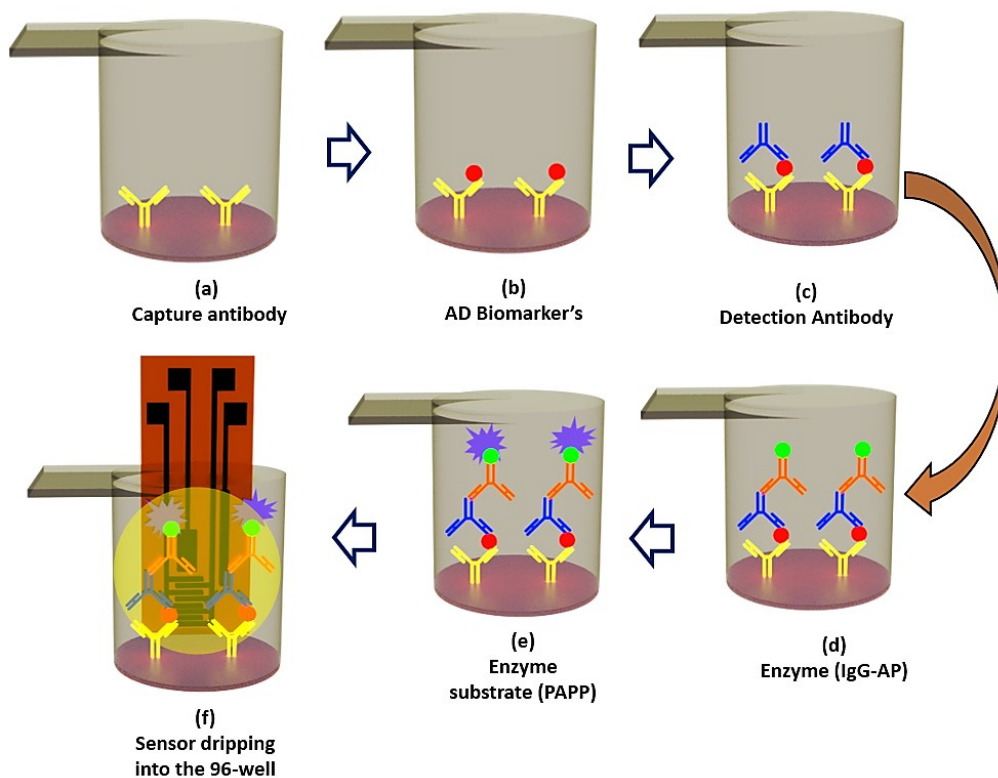## 2. Electrical characterization of the CNT-MGH n-IDA sensor

It is essential to optimize the CO2 laser parameter to achieve optimal graphene formation throughout the laser irradiation process. **Fig. S2 (a)** demonstrates that graphene formation increases correspondingly as the laser power increases; the electrical resistance decreases towards 5.4W and then becomes saturated, and the laser speed remains constant at 80 mm/sec. The proposed sensor utilizes an optimized 5.6 watts. Additionally, the electrical resistance becomes saturated at speeds below 80 mm/sec. Then, it increases proportionally to the laser speed while the power of the laser remains constant at 5.4 W, as shown in **Fig. S2 (b)**. The electrical conductivities

were calculated by applying the subsequent equation to the sheet resistance and electrode thickness.[3]

$$\text{Electrical conductivity (S/cm)} = \frac{1}{\text{Sheet resistance (Ohm per cm) X thicknmess (cm)}} \qquad \text{(i)}$$

The electrode thickness of the CNT-MHG n-IDA 8-well sensor was determined to be 32 µm, while the bare graphene sensor was 30 µm. The CNT-MHG n-IDA structure becomes more conductive when AgNPs and CNTs are added due to the increased surface area. As shown in Fig. S2 (c), the electrical conductivity of graphene containing CNTs and AgNPs is five times that of bare graphene.

3. Principle of Electrochemical ELISA (e-ELISA)

(a)
Capture antibody

(b)
AD Biomarker's

(c)
Detection Antibody

(f)
Sensor dripping
into the 96-well

(e)
Enzyme
substrate (PAPP)

(d)
Enzyme (IgG-AP)

Fig.S3. Schematic illustration e-ELISA principle and electrochemical redox cycle of PAP on IDA electrodes

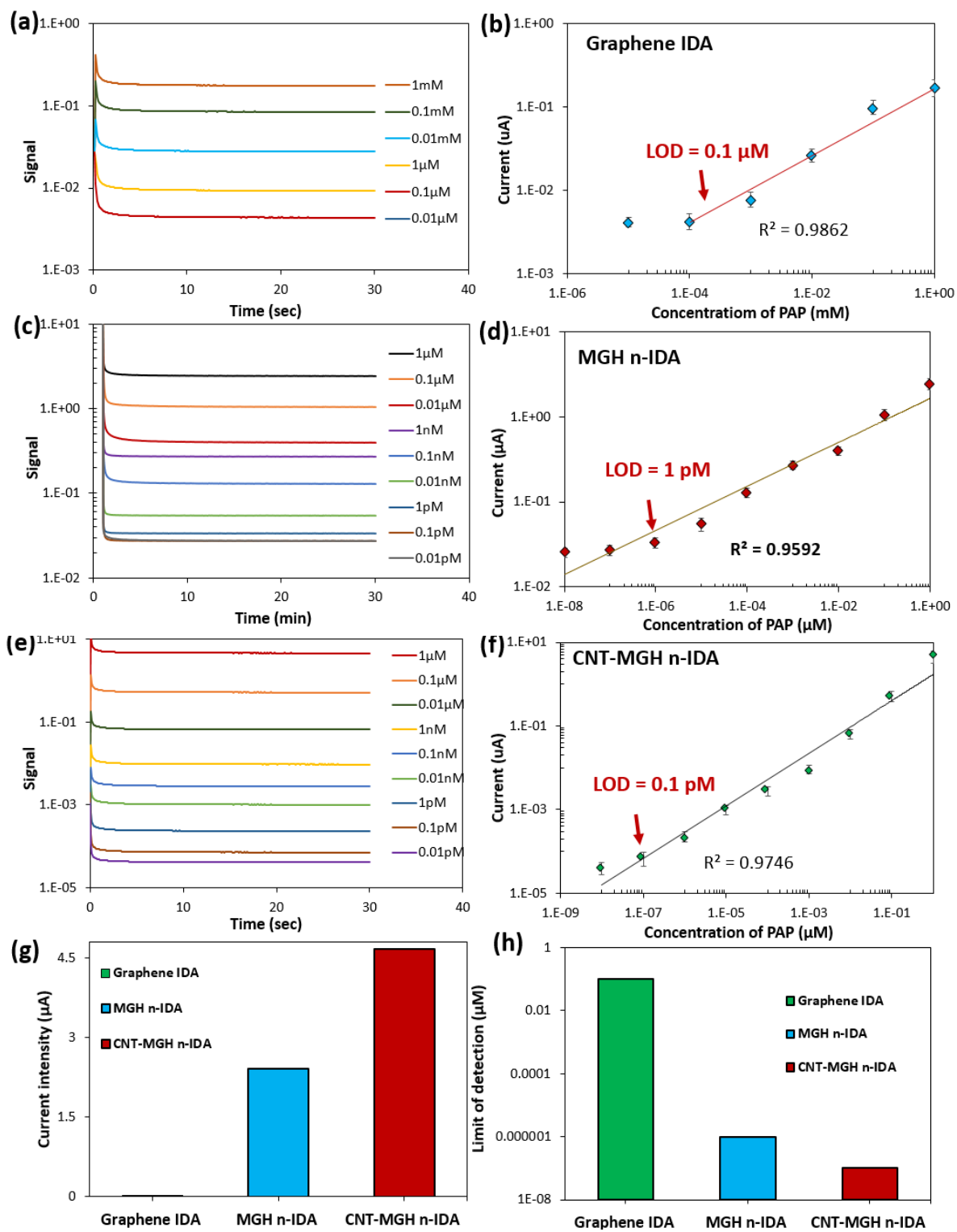## 4. Comparison of sensitivity among the proposed sensor, Graphene IDA and MGH n-IDA

Fig.S4. Comparison of sensitivity amoung the proposed sensor, Graphene IDA and MGH n-IDA,

(a~b) measured signal and Current changes of graphene IDA 8-well sensor for the different

concentration of PAP under the optimized condition, **(c~d)** measured signal and linear relationship of MGH n-IDA for different concentration of PAP, **(e~f)** measured signal and Current changes of proposed sensor for the different concentration of PAP under the optimized condition, **(g)** comparison of current intensity of proposed sensor with Graphene IDA and MGH n-IDA and **(h)** comparison of limit of detection of proposed sensor with Graphene IDA and MGH n-IDA.

## 5. Stability and Reproducibility of Developed CNT-MGH n-IDA 8-well
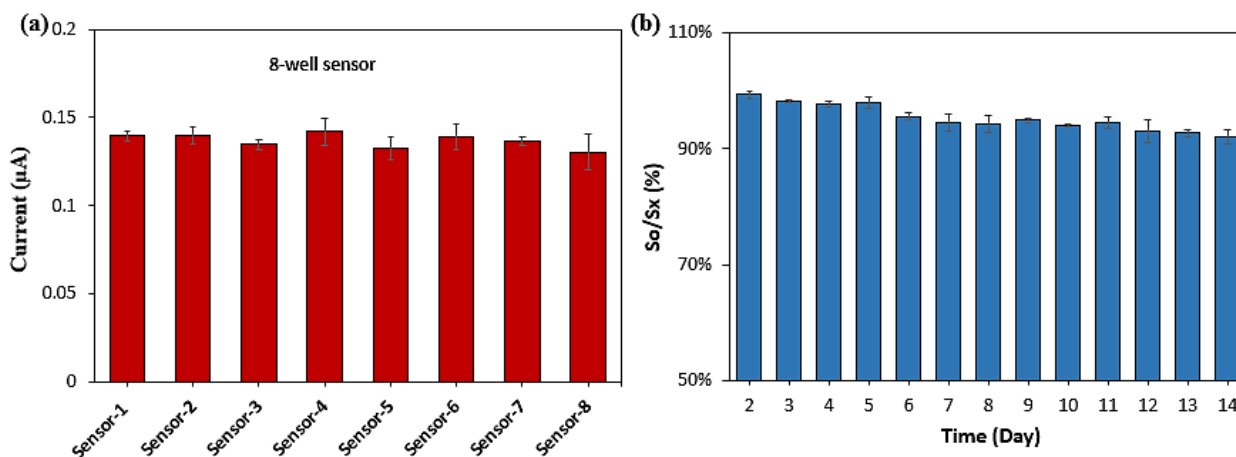
Fig. S5: **(a)** Reproducibility of 8-well sensor for 5 pg/ml p-Tau 181, **(b)** Stability of the proposed sensor (repeated experiments were conducted for 14 days).

Fig. S5(a) shows the reproducibility was investigated using one 8-well sensors with 5 pg/ml concentration of p-Tau 181 under the ambient e-ELISA experimental conditions. The 8-well sensors indicated higher reproducibility and the relative standard division was reported at 1.80%. High reproducibility ensures that 8-well sensors provide consistent and reliable measurements, which is crucial for applications requiring precise and accurate monitoring. Therefore, the proposed sensors are capable to measure multiple analytes simultaneously. Moreover, the stability was calculated by (S_0/S_x) x 100, whereas S_0 is the first-day output single and S_x represents the output signal on day x.[4] As seen in **Fig. S5 (b)**, the stability is more than 98% beyond five days and then decreases to 92% within 14 days. The above discussion indicates the proposed 8-well

sensor high stability and ensures consistent performance over time, which is crucial for long-term diagnosis of AD.

6. Experimental Procedures of Conventional ELISA and Comparative analysis for proposed sensor and Conventional ELISA.
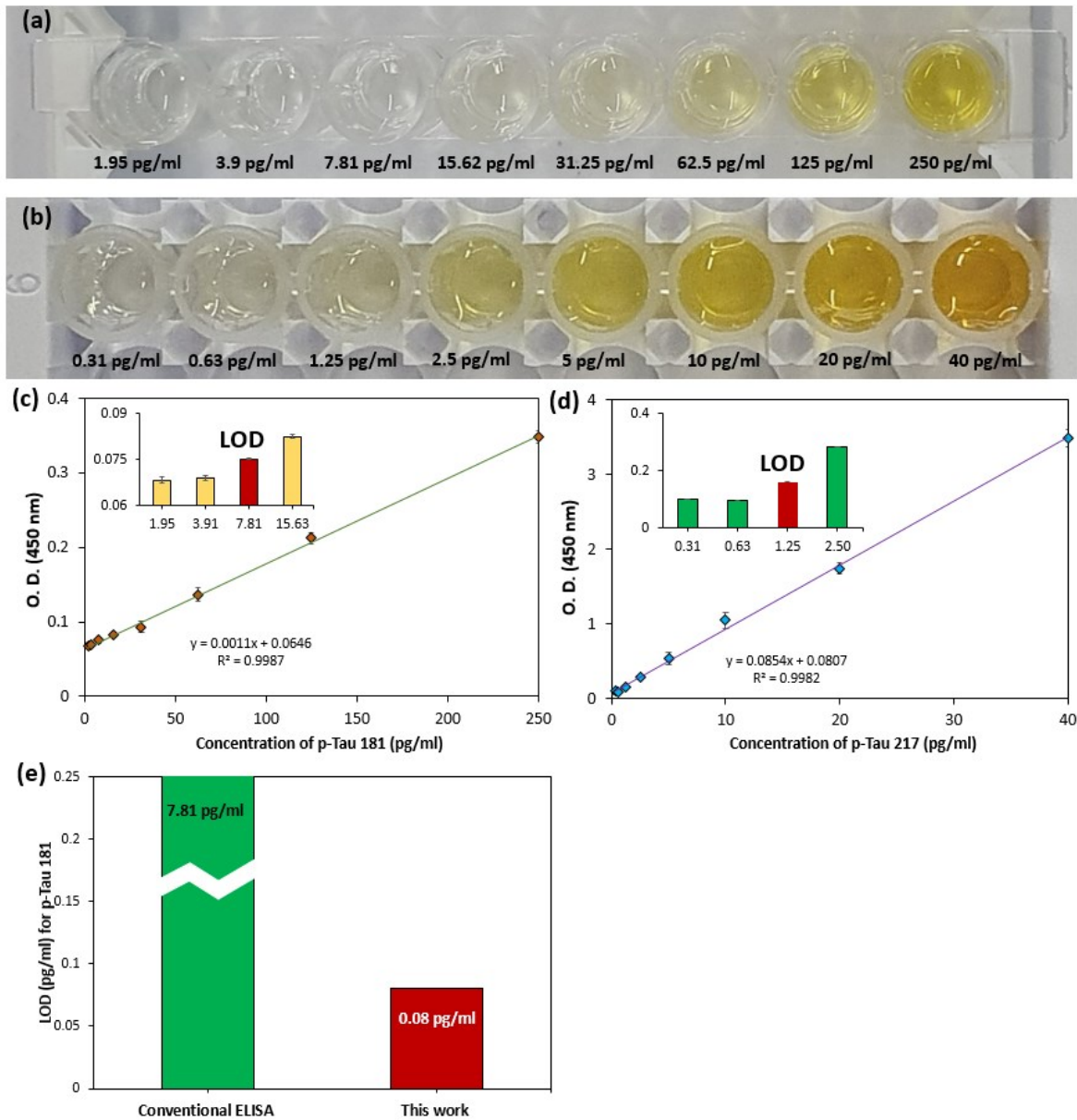
Fig. S6. Conventional ELISA, **(a)** digital image for diferrent concentrations of p-Tau 181, **(b)** digital image for diferrent concentrations of p-Tau 217, **(c)** colorimetric changes of p-Tau 181 for different cocentration, (d) colorimetric changes of p-Tau 271 for different cocentration, **(e)**

measured limit of detection (LOD) for conventional ELISA and e-ELISA with proposed electrochemical 8-well sensor for p-Tau 181.

The sandwich ELISA (Enzyme-Linked Immunosorbent Assay) is a highly specific and sensitive method used for detecting and quantifying antigens in a sample. The principle of the sandwich ELISA involves capturing the target antigen between two layers of antibodies: the capture antibody and the detection antibody.[5, 6] The procedure begins with the capture antibody, which is specific to the antigen of interest, being immobilized on the surface of a capture antibody-coated 96-well microplates. 100 µl of target antigen has been loaded to 96-well microplates followed by 2 hrs incubation at room temperature therefore, the target antigen binds to the capture antibody. Then, the microplates were washed to remove the non-specially bound antigen using 260 µl of 1x wash buffer. After that, the 100 µl of detection antibody was loaded onto each 96-well microplate, incubated for 1 hour at room temperature, and then thoroughly washed with 260 µl of the same wash buffer. The IgG-HRP (1X) was applied to the 96-well. Subsequently, the post-incubated microwell for 30 min at room temperature was thoroughly washed with 260 µl of wash buffer, 100 µl of stabilized chromogen (TNB) solution was supplied to the 96-well microplate and waited for 30 min to ensure a significant enzymatic reaction that being to turn blue signal, often a color change, which is directly proportional to the amount of antigen present in the sample. Finally, 100 µl of stop solution was added to the 96-well microplate, the solution in the 96-ewlls changes from blue to yellow as shown in the **Fig. S6 (a~b)**. The optical signal was measured for p-Tau 181 and p-Tau 217 at 450 nm optical density using DS2 Automated ELISA system, (purchased from Dynex Technologiess, Inc. USA).The measured LOD of p-181 is 7.81 pg/ml, and p-217 is 1.25 pg/ml as shown in the **Fig. S6 (c~d)** respectively. The proposed sensor has measured the lower LOD, which is almost 100 times lower than the conventional ELISA as shown in the **Fig. S6 (e)**.

Table: Comparison of LODs of the novel CNT-metal graphene hybrid Nano-IDA sensor to other benchmark sensors.

Electrode	Electrode Fabrication methods	Electrode Materials	Measurements method		Linear range	LOD	Ref.
IDA chain-shaped electrode	Conventional lithography	Gold	Immobilizing specific anti-amyloid-β (aβ) antibody onto electrode surface		10^{-3} to 10^3 ng/ml	100 pg/ml	**[7]**
			Detection technique	Electrochemical			
Commercially available SPE	Electrode surface modification	MWCNT-PAH /Pt	Antibody functionalized onto electrode surface		8.6 to 1100 pg/mL	0.24 pg/mL	**[8]**
			Detection technique	Electrochemical			
screen printed graphene electrodes	Electrode modification	Ultra-thin pDAN/ DAN	Antibody functionalized onto electrode surface		1 to 1000 pg/ml	4.25 pg/ml	[9]
			Detection technique	Electrochemical			
Feld-effect transistors (FETs)	Photolithography	thin SiO2 dielectric layer	aptamer-functionalized		0.1 pg/ml to 10 µg/ml	---	[10]
			Detection technique	random telegraph signal			
mini-pillar-based electrochemical sensor	PDMS pillar fabricated by PTEE template	Nano dendrites gold	immobilizing of antibody on the gold electroplated pillar surface		10^{-10} to 10^{-7} mg/ml	8.6×10^{-12} mg/ml	[11]
			Detection technique	Electrochemical			

CNT-MGH n-IDA 8-well sensor	Laser induced Graphene (LIG)	LIG-MWCNT-AgNPs	Electrochemical ELISA (e-ELISA)	0.01pM to 1000000 pM	0.08 pg/ml	**This work**

Reference

[1]   Niwa, Y. Xu, B. H. Halsall, R. W. Heineman, Analytical chemistry, 1993, 65(11), 1559-1563.

[2]   M. Morita, K. Hayashi, T. Horiuchi, S. Shibano, K. Yamamoto, J. K. Aoki, Journal of the Electrochemical Society, 2014, 161(4), H178.

[3]   A. M. Zahed, C. S. Barman, S. P. Das, M. Sharifuzzaman, S. H. Yoon, Y. J. Park, Biosensors and Bioelectronics, 2020, 160, 112220.

[4]   E. S. Yulianti, S. F. Rahman, M. Rizkinia, A. Zakiyuddin, *Arabian Journal of Chemistry*, 2024, *17*(4), 105692.

[5]   S. Aydin, Peptides, 2015, 72, 4-15.

[6]   J. A. Asturias, M. C. Arilla, M. Aguirre, N. Gomez-Bayon, A. Martınez, R. Palacios, F. Sanchez-Gascon, J. Martınez, Journal of immunological methods, 1999, 229(1-2), 61-71.

[7]   H. T. N. Le, J. Park, S. R. Chinnadayyala, S. Cho, Biosensors and Bioelectronics, 2019, 144, p.111694.

[8]   M.E. Schneider, L. Guillade, M.A. Correa-Duarte, F. T. Moreira, Bioelectrochemistry, 2022, 145, 108057.

[9]   H. Y. Abbasi, Z. Tehrani, A. Devadoss, M. M. Ali, S. Moradi-Bachiller, D. Albani, O. J. Guy, *Nanoscale Advances*, 2021, *3*(8), 2295-2304.

[10]   Y. Kutovyi, H.   Hlukhova, N. Boichuk, M. Menger, A. Offenhäusser, S. Vitusevich, Biosensors and bioelectronics, 2020, 154, 112053.

[11]   Y. Song, T. Xu, Q. Zhu, X. Zhang, Biosensors and Bioelectronics, 2020, 162, 112253.